

Radiation Pressure Acceleration by Ultraintense Laser Pulses

Tatiana V. Liseykina^{1,2}, Andrea Macchi^{3,4}, Sara Tuveri⁴

¹ Max-Planck Institute for Nuclear Physics, Heidelberg, Germany

E-mail: Tatyana.Liseykina@mpi-hd.mpg.de

² Institute of Computational Technologies SD RAS, Novosibirsk, Russia

³polyLab, CNR-INFM, Pisa, Italy

⁴Dipartimento di Fisica “Enrico Fermi”, Pisa, Italy

Abstract. The future applications of the short-duration, multi-MeV ion beams produced in the interaction of high-intensity laser pulses with solid targets will require improvements in the conversion efficiency, peak ion energy, beam monochromaticity, and collimation. Regimes based on Radiation Pressure Acceleration (RPA) might be the dominant ones at ultrahigh intensities and be most suitable for specific applications. This regime may be reached already with present-day intensities using circularly polarized (CP) pulses thanks to the suppression of fast electron generation, so that RPA dominates over sheath acceleration at any intensity. We present a brief review of previous work on RPA with CP pulses and a few recent results. Parametric studies in one dimension were performed to identify the optimal thickness of foil targets for RPA and to study the effect of a short-scalelength preplasma. Three-dimensional simulations showed the importance of “flat-top” radial intensity profiles to minimise the rarefaction of thin targets and to address the issue of angular momentum conservation and absorption.

PACS numbers: 52.38.Dx, 52.38.Kd, 52.38.Rr

Submitted to: *Plasma Phys. Control. Fusion*

1. Introduction

In 1966, a paper in *Nature* by G. Marx [1] considered the possibility to travel into outer space using a rocket propelled by an Earth-based laser beam. The concept was as simple as follows: the rocket's engine and fuel are replaced by a mirror, and the force exerted on the mirror due to the radiation pressure of the laser light boosts the rocket. Although, obviously, a prototype of such rocket has never been realized so far (and probably will never be), Marx's paper outlined the idea that the *efficiency* of the system, i.e. the ratio between the mechanical energy of the object accelerated by the laser beam and the energy contained in the laser beam itself, would approach unity as far as the velocity of the object approaches the speed of light. An heuristic (though incomplete) argument might be given in terms of light quanta, i.e. photons, although the system can be described as entirely classical: let us consider a "perfect" mirror irradiated by a monochromatic light wave of frequency ω , that contains a certain number N of photons and thus has a total energy $N\hbar\omega$. The mirror reflects photons conserving their number in any frame. If the mirror has an (instantaneous) velocity $V = \beta c$ in the laboratory frame, the frequency of the reflected photons is $\omega' = \omega(1 - \beta)/(1 + \beta)$. Thus, since N is invariant, the energy of the reflected pulse tends to zero if $V \rightarrow c$, so that a mirror moving at a speed close to c absorbs almost all the energy of the incident pulse.

Marx paper's conclusions turned out to be right although its approach needed a critical revision, as can be found in the rigorous and pedagogical description of Ref.[2]. According to the formulas in Ref.[2]. it would take a 3 yr time for a 10 TW laser to accelerate a 10^3 kg rocket to $V = (4/5)c$. Scaling this result to the typical parameters of superintense laser pulses and micro-targets, we obtain that about 5×10^{10} Carbon ions might be accelerated to the same speed in 1 ps by a 1 PW laser, which is within the capabilities of present technology. This makes the perspective of Radiation Pressure Acceleration (RPA) attractive for applications requiring large numbers of relativistic ions.

Nearly all of the experiments reported in the last decade on the acceleration of ions (mainly protons) by superintense laser pulses (see e.g. [3, 4] and refs. therein) are not based on RPA but instead on the Target Normal Sheath Acceleration (TNSA) mechanism, in which ions are accelerated by space-charge fields created by multi-MeV electrons escaping in vacuum. The dominance of RPA over TNSA in thin solid targets irradiated at intensities higher than those of present-day experiments has been claimed by Esirkepov and coworkers [5, 6], on the basis of simulations showing a transition occurring at some intensity value above 10^{21} W cm $^{-2}$, with a strong dominance leading to the so-called "piston" regime over 10^{23} W cm $^{-2}$. Such an intensity may be available only in several years from now thanks to the development of advanced laser facilities. Experimentally, a preliminary indication of RPA effects in thin targets at intensities approaching 10^{20} W cm $^{-2}$ has been published recently [7] (some experimental results on ion acceleration at intensities $\leq 10^{18}$ W cm $^{-2}$ were also interpreted in terms of purely ponderomotive effects [8]).

The question then arises whether it is possible to achieve a RPA-dominated regime already at lower intensity; this corresponds in practice to quench the generation of high-energy electrons, as these latter drive TNSA but do not contribute to RPA. This is actually possible using circularly polarized (CP) laser pulses at normal incidence because the *oscillating* components of the Lorentz force in the direction perpendicular to the sharp density gradient vanish (for a plane wave) or are relatively small (for a finite laser spot size): as a consequence, the motion of electrons at the interaction surface is adiabatic and electron heating is strongly reduced, while the space-charge field created to balance the local radiation pressure (i.e. the ponderomotive force) accelerates ions.

The strong differences between the cases of linearly polarized (LP) and CP pulses have been evidenced in some papers by our group [9, 10] mostly for the case of “thick” targets, much deeper than the skin layer in which the laser pulse penetrates. These studies showed that for CP the interaction accelerates all the ions in the skin layer and the fastest ones produce a very dense “bunch” with a narrow energy spectrum, directed in the forward direction.

Recently, the experimental availability of ultrathin targets (i.e. with thickness down to a few nanometers) and high-contrast laser pulses suggested the study of CP-RPA with such pulses and targets. The simulations performed independently by several groups [11, 12, 13, 14, 15] suggest that indeed the whole target may be accelerated leading to efficient generation of large numbers of ions with monoenergetic spectra in the near-GeV range. Presently, no experiment using CP pulses at normal incidence has been reported in publications yet, but several related proposals have been made, so that the CP-RPA concept is expected to be explored soon.

The present paper reviews the main issues of CP-RPA and reports novel numerical results on parametric studies in one spatial dimension (1D), showing the role of the target thickness and the case of RPA in short-scalelength preformed plasmas, as well as first results in fully 3D geometry where, in particular, the issue of angular momentum conservation can be addressed.

2. Theory and earlier work

A physical description and a simple model of RPA in thick targets (assuming a priori non-relativistic ions) has been given in previous work [9, 16]. Briefly, electrons pile up quickly in the skin layer due to the action of the ponderomotive force, until the latter is balanced by the charge separation field that accelerates the ions. These latter produce a sharp density spike at the end of the skin layer where hydrodynamical breaking occurs, with the faster ions creating a dense bunch (with narrow spectrum) that moves ballistically into the plasma (a rather similar dynamics has been noted in the case of radial ponderomotive acceleration of ions in an underdense plasma [17]). A simple model provides the following scaling (valid for sub-relativistic ion velocities) for the maximum ion velocity and the corresponding energy (which almost corresponds to the

bunch velocity):

$$\frac{v_{im}}{c} = 2\sqrt{\frac{Z m_e n_c}{A m_p n_e}} a_L, \quad \mathcal{E}_m = \frac{m_i}{2} v_{im}^2 = 2m_e c^2 Z \frac{n_c}{n_e} a_L^2, \quad (1)$$

where $n_c = m_e \omega^2 / 4\pi e^2 = 1.1 \times 10^{21} \text{ cm}^{-3}$ is the cut-off density for the laser wavelength $\lambda = 2\pi c / \omega$, n_e is the background electron density, $a_L = eE_L / m_e \omega c = 0.85(I\lambda^2 / 10^{18} \text{ W cm}^{-2})$ is the dimensionless amplitude of the laser pulse with electric field E_L and intensity I , and other symbols are standard. Actually, this result has been derived in the limit of relatively low intensity but, surprisingly, this scaling has been found to hold up to much higher intensity in parametric 1D simulations [16].

The ion bunch is formed in a time of the order of $\sim c / \omega_p v_{im}$ (where ω_p is the plasma frequency) after which it exits the skin layer accompanied by neutralizing electrons, and the laser pulse may accelerate a new layer. If energies higher than the above estimate must be reached, it is necessary to repeat the acceleration stage on the same ions, i.e. the target must be thin enough in order that all the ions are bunched and accelerated via several cycles. Simulation results on the acceleration of ultrathin targets have been interpreted with the model of the accelerating mirror [13] where the latter is assumed to be a “rigid” object, neglecting its internal dynamics.

Although a few authors have proposed the RPA of a thin foil as a way to generate high-energy protons, this approach seems to be most interesting for the acceleration of higher- Z ions. In fact, while it seems technologically unfeasible to have an ultrathin target made of hydrogen only, in a multiple species target all the ions will be accelerated to the same velocity, resulting in higher energies for the heavier species. If a lighter species (e.g., hydrogen) is present, these ions will be first accelerated overturning the heavier ones, but this will cause them to decouple from the laser pulse, the latter being screened by the heavier ion layer. These latter will be accelerated until they reach the lighter ions allowing the laser to reach them and accelerate them further, but as the result of a “long” acceleration all species will have the same velocity. This effect also ensures that for an ultrathin target of a single species material (e.g., Carbon) the ion spectrum will tend to be monoenergetic.

The above picture of the acceleration dynamics should change when the ion finally reach a speed close to c , as they will no longer be separated by electrons. The “laser-piston” regime investigated by Esirkepov et al [5] corresponds to conditions in which the ions are promptly accelerated to relativistic velocities and stick to the electrons, which may not be assumed to be in a mechanical quasi-equilibrium anymore. In the present paper we restrict our analysis to the regime of non-relativistic ions because near-term experiments on RPA will unlikely have the potential to accelerate ions up to strongly relativistic energies.

The theoretical picture and the predicted scalings have been supported by 1D simulations. So far multi-dimensional effects have been addressed at most by 2D simulations for both thick [9, 10, 16] and thin [13, 14, 15] targets. In the thick target cases, the energy spectrum is basically determined by the convolution of the 1D scaling

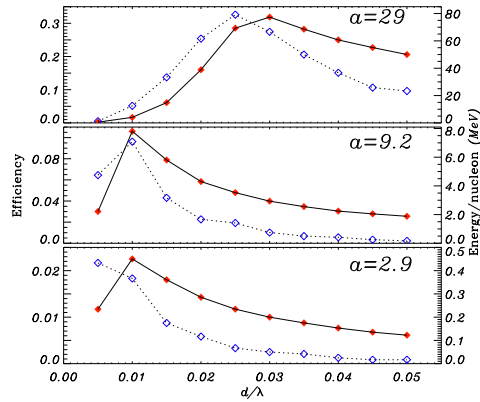


Figure 1. Energy conversion efficiency into ions (red filled diamonds) and the “peak” energy per nucleon (blue empty diamonds) as a function of the target thickness, investigated by parametric 1D PIC simulations. The top, middle and bottom plots are for a pulse amplitude $a = 29, 9.2$ and 2.9 , respectively. In all the runs, the laser pulse had a duration of 9 cycles (FWHM), the electrons density was $n_e = 250n_c$ and the charge-to-mass ratio was $Z/A = 1/2$.

law with the intensity profile of the pulse. The angle of emission of ions is energy-dependent, but overall a good collimation is already obtained for a Gaussian pulse profile [10]. For thin targets, use of a flat-top profile increases monoenergeticity and collimation, also keeping a low heating of electrons, as expected [13, 14].

The issue of target stability during RPA has been addressed in thin foil 2D simulations for CP [14] and also for linear polarization in the ultraintense regime [18], showing a bending instability which has been interpreted to be of the Rayleigh-Taylor type and hence can be described in terms of the radiation pressure only. Simulations for thick targets, however, have shown that surface instabilities are weaker for CP pulses than for linearly polarized ones, with the quality of the ion beam possibly becoming poorer in the latter case [16].

3. 1D simulations

3.1. The role of the target thickness

We performed a parametric study to determine the optimal values of target thickness d to obtain higher efficiency and/or ion energy for given laser parameters. In order to be able to cover a quite wide range of parameters and to simulate “realistic” target densities we used 1D simulations, which in the CP-RPA regime have so far proved to yield efficiency and ion energy values close to those from 2D or 3D simulations for those cases where a comparison is possible (i.e. for moderate density values). Results are shown in Fig. 1. The electron density of the target and the pulse duration were kept constant for all runs and corresponded, for a laser wavelength $\lambda = 0.8 \mu\text{m}$, to $n_e = 4.3 \times 10^{23} \text{ cm}^{-3}$ and $\tau_L = 24 \text{ fs}$. The three values of the dimensionless amplitude that were studied ($a = 2.9,$

9.2 and 29) corresponded to intensities $I = 1.8 \times 10^{19}$, 1.8×10^{20} and 1.8×10^{21} W cm⁻², respectively.

The values of d for which efficiency and ion energy have their maximum are close to each other and, as expected, they correspond to ultrathin, sub-micrometric targets. The strong decrease of efficiency and energy for smaller values of d may be explained with the onset of relativistically induced transparency in the thin foil when $d \simeq \lambda a(n_c/n_e)$ [19], so that the total radiation pressure on the target decreases. This point will be further discussed below when addressing three-dimensional effects (section 4).

The energy per nucleon reported in Fig. 1 can be scaled to all species with $Z/A = 1/2$. For Carbon ($A = 12$) the highest energy of 0.96 GeV is obtained for $a = 29$ and $d = 0.025\lambda$. Notice that these are “peak” energies which correspond to a distinct maximum in the ion spectra. However, depending on the interaction parameters some tail of higher energy ions appears. Moreover, the width of the ion energy peak also varies throughout the simulations and does not remain constant in time, as some broadening is observed after the laser pulse is over. This broadening appears to be related with electron heating which occurs at the end of the acceleration stage, creating “warm” electrons which are much less energetic than those produced for LP interaction but may already drive the expansion of the thin plasma foil. Hence, monoenergeticity of ions appears to be a non trivial issue already in 1D.

In higher dimensionality it is known that the intensity distribution in the laser spot gives rise to an energy spread correlated with the direction of laser-accelerated ions [10], so that a “flat-top” distribution, whenever feasible, may improve monoenergeticity as well as beam collimation (see e.g. 2D simulations in Ref.[13]). Additional effects of the pulse profile are also discussed in section 4.

3.2. RPA in preformed plasmas

The use of ultrathin targets in experiments will require the use of systems with an extremely high contrast ratio, otherwise the prepulse preceding the main interaction pulse will destroy the target completely. Interaction experiments in such regime appears to be presently possible, thanks e.g. to the use of plasma mirrors to improve the contrast [20]. Such conditions are optimal to test the CP-RPA of ultrathin targets, provided that the strategies implemented to improve the pulse contrast are compatible with preserving the circular polarization of the pulse. It is also worth to stress that the need of normal pulse incidence might also be non trivial due to the danger of back-reflection from the overdense plasma.

It is interesting in any case to consider the possibility of the interaction of the CP pulse with a non-uniform preplasma, as these may be the actual conditions in experiments where the contrast ratio is not extremely high. Moreover, the expected scaling of the ion energy with the inverse of the plasma density suggests that, in a preformed plasma, a given laser pulse may produce a lower total number of ions but with higher energy, as the interaction occurs with the layer at the cut-off density n_c

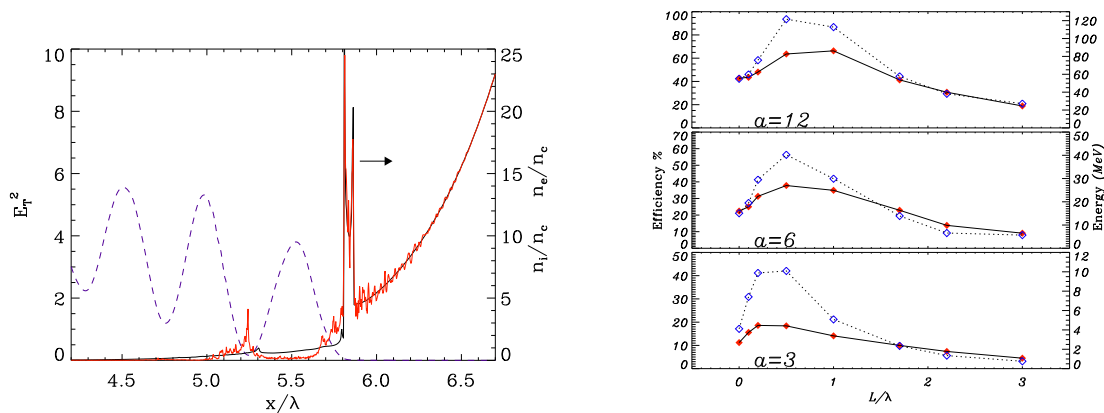


Figure 2. Interaction with preformed plasmas. Left: snapshots of the profiles of $E_T^2 = E_y^2 + E_z^2$ (dashed blue line), n_i (thick black line) and n_e (thin red line) soon after the formation of the “fast” ion bunch (evidenced by the arrow). The pulse intensity was $a = 3$ corresponding to $1.2 \times 10^{19} \text{ W cm}^{-2}$ for $\lambda = 1 \mu\text{m}$. Right: conversion efficiency (red filled diamonds, solid line) and peak energy (blue empty diamonds, dashed line) of ions as a function of the density scalelength L , for three values of the laser amplitude a . In all the simulations the laser pulse had a duration of 9 cycles (FWHM) and the density profile was rising with a $\sim (x - x_0)^4$ law up to a peak density $n_0 = 16n_c$, and then remained constant.

which is typically less than one hundredth of the solid density.

We performed a set of parametric 1D simulations assuming initial density profiles of power-law type (i.e. $n_0(x) \sim (x - x_0)^k$ for $x > x_0$) and different values of the density scalelength at the cut-off layer, $L = n_c/|\partial_x n_0|_{n_0=n_c}$. The snapshot of the ion density in Fig.2 shows that the ion density spiking, breaking and formation of a “fast” bunch occur near the critical density layer, with features very similar to the case of a sharply rising density (no preplasma) [9]. The bunch density is several times n_c . As a function of L , both the maximum ion energy and the conversion efficiency have their maxima for a very short scalelength $L \simeq 0.5\lambda$, as also shown in Fig.2 where $L = 0$ corresponds to the case of no preplasma, i.e. a step-like profile. When compared to the energy scaling (1), the observed ion energy would correspond to a density value intermediate between n_c , and the peak density ($16n_c$) of the profile. Decrease of energy and efficiency for larger values of L might be related to worse coupling of the laser pulse with the cut-off layer; in Fig.2 we observe that, near the first null point of the standing wave created by the reflection of the pulse, electrons pile up under the action of the ponderomotive force creating an overdense layer for the rest of incoming pulse. A broader energy spectrum is also observed for non-optimal values of L ; Fig.2 reports the maximum or cut-off energy, but several and broad “peaks” may appear in the spectrum in such conditions, while the spectrum is narrow for the case of absolute maximum energy. These preliminary results suggest that, while RPA may be strongly affected by prepulse effects, control of the latter may allow to achieve dense bunches of multi-MeV ions using ultrashort pulses with controlled contrast. For longer pulses (hundreds of fs), this approach may become ineffective because of strong steepening effects during the rise of the pulse, decreasing

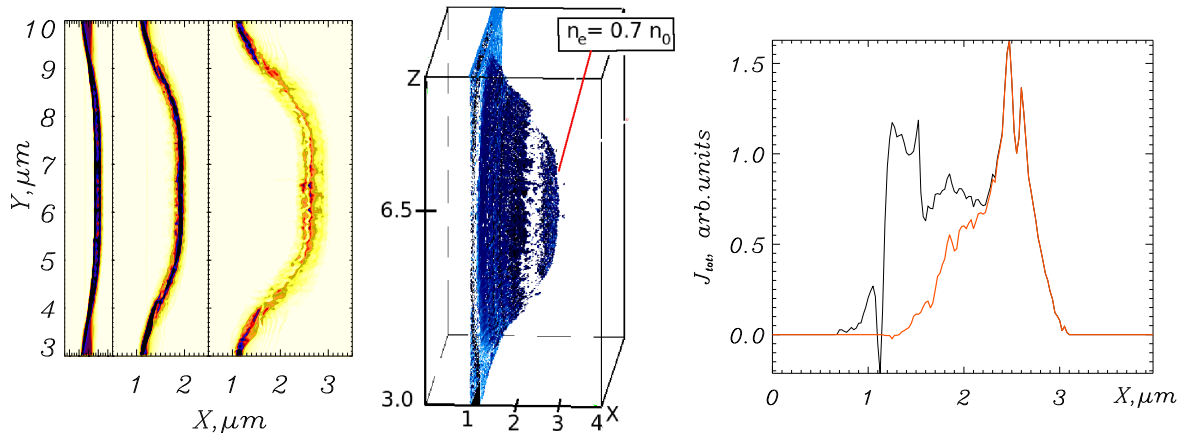


Figure 3. 3D simulations. Left: the distribution of ion density at $t = 75, 100$ and 130 fs in (xy) plane; middle: the distribution of the ion density at $t = 130$ fs (the laser pulse is over); right: the integral of the ion poloidal current $\oint J_{\phi} dy dz$ at $t = 130$ fs versus longitudinal coordinate, showing the angular momentum absorption: black line - for the region with radius $r = 4.5 \mu m$ around the x axis; red line - for the $r = 2.5 \mu m$ region around the x -axis.

the value of L_c . The width of the target layer that remains undamaged from the prepulse may also play a role because the ions may undergo relevant collisional losses crossing the solid-density region (see e.g. the discussion in [7]).

4. 3D simulations

As it is always the case for computational plasma physics, 3D simulations would be required for a “realistic” description, but the limits of computing power forces the restriction to a narrow set of “feasible” parameters. This is the case for CP-RPA where, furthermore, the resolution must be high enough to resolve effects such as the strong spiking of the density observed in 1D and 2D. Thus, only a few 3D runs could be performed and for plasma densities much less than solid-density values, though well above n_c .

The comparison with 1D and 2D cases is important also because a CP pulse carries a net angular momentum whose conservation law appears as an additional constraint in 3D. To this point we notice that, despite the strong absorption of the pulse energy in CP-RPA at high intensities, as far as the acceleration takes place adiabatically, as it is the case for the “perfect mirror” model, *no* absorption of angular momentum is expected. In fact, coming back to the heuristic argument of the introduction, if the number of photons is conserved and the reflected beam conserve its helicity (that can be shown to hold), no angular momentum is left in the target because the “spin” of any photon is \hbar independently of the frequency.

In order to address these topics, we performed several 3D simulations. In all the runs discussed here the normally incident laser pulse was circularly polarized with a peak intensity of $3.4 \times 10^{19} \text{ W cm}^{-2}$ and ~ 60 fs duration and the target was consisting of

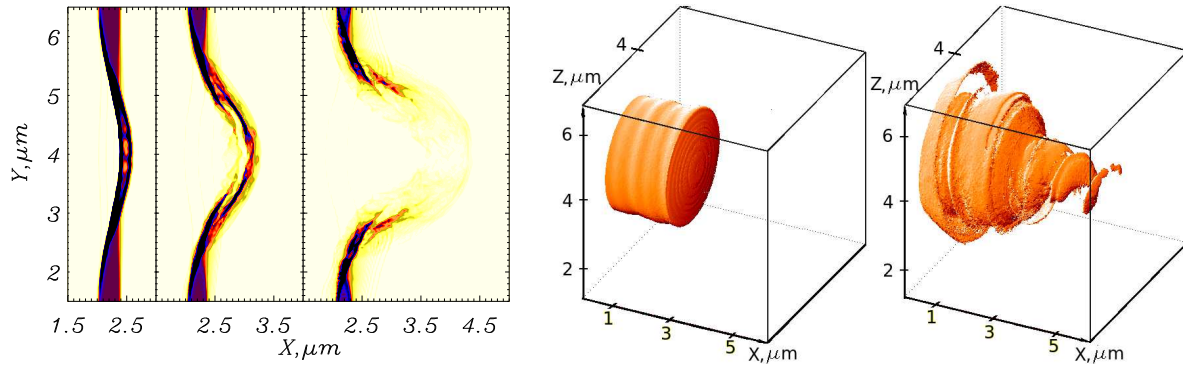


Figure 4. 3D simulations. Left: the distribution of ion density at $t = 75, 100$ and 130fs ; right: the distribution of the electromagnetic energy at $t = 50\text{fs}$ and $t = 100\text{fs}$ in the case of tiny ($3\mu\text{m}$ width) laser pulse interaction with ultrathin foil.

electrons and protons. Fig. 3 presents the results of the interaction of a laser pulse with a “flat-top” intensity profile of $6\mu\text{m}$ width with a target of density $n_e = 16n_c = 1.7 \times 10^{22}\text{cm}^{-3}$ and $0.3\mu\text{m}$ thick. Fig. 3 (a) shows the 2D distributions of ion density at $t=75, 100$ & 130fs , and Fig. 3 (b) – the 3D plot of the ion density the when the laser pulse is over. The density of the “bunch” is approximately 0.7 of the initial density of the target, the peak energy of ions in this bunch is $\sim 4\text{MeV}$, the number of accelerated protons is $\sim 4 \times 10^{10}$. This is the case when some degree of the angular momentum absorption is observed, and when the laser pulse is over the most of the absorbed angular momentum ($\sim 4\%$) is transferred to the protons (the energy absorption in this case was $\sim 7\%$). To prove that a torque on the plasma ions exist, we plot in Fig. 3 (c) the integral (in (y,z)) of the poloidal current J_φ of the ions. We thus see that on the average there is a net “rotation” of the ions, while the same plot for the electron current shows that the latter averages over x almost to zero. The observation of some degree of angular momentum absorption is a signature of non-adiabatic or “dissipative” effects, which are an interesting issue in collisionless systems, and in the specific case of CP-RPA may be related to the onset of hydrodynamical breaking during the acceleration process, violating the adiabaticity condition.

In Figs. 4 the results of the simulation of the interaction of a tiny ($3\mu\text{m}$ width) Gaussian laser pulse with the target of density $n_e = 9n_{cr} = 1 \times 10^{22}\text{cm}^{-3}$ and thickness of $0.4\mu\text{m}$ are shown. In this case the pulse was tiny enough to contribute dramatically to the induced transparency of the target.

In both cases presented here the density and the width of the targets were chosen in the way to ensure their opacity on the basis of the 1D analysis. However, as far as the 3D effects contribute to decrease the transparency threshold (because the foil tends to expand in perpendicular direction) for the tiny gaussian laser pulse this effect was much more pronounced so that the foil became transparent even if initially opaque. Since the use of the target with densities non very far from the transparency threshold is more suitable to achieve the efficient acceleration rate, the shape of the laser pulse becomes

a critical issue and the use of a “flat-top” distribution laser pulses, whenever possible, may help.

Acknowledgments

This work was supported by CNR-INFN and CINECA (Italy) through the super-computing initiative and by CNR via a RSTL project. Part of the work was performed during a stay of two of the authors at Queen’s University, Belfast, UK, supported by a Visiting Research Fellowship (A.M.) and by COST-P14 (S.T.). One of the authors (T.V.L.) also acknowledge the support RFBR (via 08-02-0844 grant).

References

- [1] G. Marx. Interstellar vehicle propelled by terrestrial laser beam. *Nature*, 211:22–23, 1966.
- [2] J. F. L. Simmons and C. R. McInnes. Was Marx right? or How efficient are laser driven interstellar spacecraft? *American Journal of Physics*, 61(3):205–207, 1993.
- [3] M. Borghesi, J. Fuchs, S. V. Bulanov, A. J. MacKinnon, P. K. Patel, and M. Roth. Fast ion generation by high-intensity laser irradiation of solid targets and applications. *Fus. Sci. Techn.*, 49:412, 2006.
- [4] P McKenna, F Lindau, O Lundh, D C Carroll, R J Clarke, K W D Ledingham, T McCanny, D Neely, A P L Robinson, L Robson, P T Simpson, C-G Wahlström, and M Zepf. Low- and medium-mass ion acceleration driven by petawatt laser plasma interactions. *Plasma Phys. Contr. Fusion*, 49(12B):B223–B231, 2007.
- [5] T. Esirkepov, M. Borghesi, S. V. Bulanov, G. Mourou, and T. Tajima. Highly efficient relativistic-ion generation in the laser-piston regime. *Phys. Rev. Lett.*, 92(17):175003, 2004.
- [6] T. Esirkepov, M. Yamagiwa, and T. Tajima. Laser ion-acceleration scaling laws seen in multiparametric particle-in-cell simulations. *Phys. Rev. Lett.*, 96(10):105001, 2006.
- [7] S. Kar, M. Borghesi, S. V. Bulanov, M. H. Key, T.V. Liseykina, A. Macchi, A. J. Mackinnon, P. K. Patel, L. Romagnani, A. Schiavi, and O. Willi. Plasma jets driven by ultra-intense laser interaction with thin foils. *Phys. Rev. Lett.*, 2008. accepted for publication.
- [8] J Badziak, S Glowacz, S Jablonski, P Parys, J Wolowski, H Hora, J Krása, L Láška, and K Rohlena. Production of ultrahigh ion current densities at skin-layer subrelativistic laser–plasma interaction. *Plasma Phys. Contr. Fusion*, 46(12B):B541–B555, 2004.
- [9] Andrea Macchi, Federica Cattani, Tatiana V. Liseykina, and Fulvio Cornolti. Laser acceleration of ion bunches at the front surface of overdense plasmas. *Phys. Rev. Lett.*, 94(16):165003, 2005.
- [10] T. V. Liseykina and A. Macchi. Features of ion acceleration by circularly polarized laser pulses. *Appl. Phys. Lett.*, 91(17):171502, 2007.
- [11] Xiaomei Zhang, Baifei Shen, Xuemei Li, Zhangying Jin, and Fengchao Wang. Multistaged acceleration of ions by circularly polarized laser pulse: Monoenergetic ion beam generation. *Phys. Plasmas*, 14(7):073101, 2007.
- [12] Xiaomei Zhang, Baifei Shen, Xuemei Li, Zhangying Jin, Fengchao Wang, and Meng Wen. Efficient GeV ion generation by ultraintense circularly polarized laser pulse. *Phys. Plasmas*, 14(12):123108, 2007.
- [13] A P L Robinson, M Zepf, S Kar, R G Evans, and C Bellei. Radiation pressure acceleration of thin foils with circularly polarized laser pulses. *New J. Phys.*, 10(1):013021, 2008.
- [14] O. Klimo, J. Psikal, J. Limpouch, and V. T. Tikhonchuk. Monoenergetic ion beams from ultrathin foils irradiated by ultrahigh-contrast circularly polarized laser pulses. *Phys. Rev. ST Accel. Beams*, 11(3):031301, Mar 2008.

- [15] X. Q. Yan, C. Lin, Z. M. Sheng, Z. Y. Guo, B. C. Liu, Y. R. Lu, J. X. Fang, and J. E. Chen. Generating high-current monoenergetic proton beams by a circularly polarized laser pulse in the phase-stable acceleration regime. *Phys. Rev. Lett.*, 100(13):135003, 2008.
- [16] T. V. Liseikina, D. Prellino, F. Cornolti, and A. Macchi. Ponderomotive acceleration of ions: circular vs linear polarization. *IEEE Trans. Plasma Science*, 2008. in press.
- [17] A. Macchi, F. Ceccherini, F. Cornolti, S. Kar, and M. Borghesi. Electric field dynamics and ion acceleration in the self-channeling of a superintense laser pulse. *Plasma Phys. Contr. Fusion*, 2008. submitted for publication.
- [18] F. Pegoraro and S. V. Bulanov. Photon bubbles and ion acceleration in a plasma dominated by the radiation pressure of an electromagnetic pulse. *Phys. Rev. Lett.*, 99(6):065002, 2007.
- [19] V. A. Vshivkov, N. M. Naumova, F. Pegoraro, and S. V. Bulanov. Nonlinear electrodynamics of the interaction of ultra-intense laser pulses with a thin foil. *Phys. Plasmas*, 5(7):2727–2741, 1998.
- [20] T. Ceccotti, A. Levy, H. Popescu, F. Reau, P. D’Oliveira, P. Monot, J. P. Geindre, E. Lefebvre, and Ph. Martin. Proton acceleration with high-intensity ultrahigh-contrast laser pulses. *Phys. Rev. Lett.*, 99(18):185002, 2007.